HHS Public Access

Author manuscript

Biochem Pharmacol. Author manuscript; available in PMC 2022 January 01.

Published in final edited form as:

Biochem Pharmacol. 2021 January ; 183: 114323. doi:10.1016/j.bcp.2020.114323.

Flightless-I is a potential biomarker for the early detection of alcoholic liver disease

Jaime Arellanes-Robledo[a,b,c,d,*], **Joseph Ibrahim**[a,b], **Karina Reyes-Gordillo**[a,b], **Ruchi Shah**[a,b,e], **Leslie Leckey**[a,b], **M. Raj Lakshman**[a,b,§]

[a]Lipid Research Laboratory, VA Medical Center. Washington, D.C., USA.

[b]Department of Biochemistry and Molecular Medicine, The George Washington University Medical Center. Washington, D.C., USA.

[c]Laboratory of Hepatic Diseases, National Institute of Genomic Medicine – INMEGEN. CDMX, Mexico.

[d]Directorate of Cátedras, National Council of Science and Technology – CONACYT. CDMX, Mexico.

[e]Cedars-Sinai Medical Center. Los Angeles, CA, USA.

Abstract

Alcoholic liver disease (ALD) is closely linked to oxidative stress induction. Antioxidant enzymes balance oxidative stress and function as intermediary signaling regulators. Nucleoredoxin (NXN), an antioxidant enzyme, regulates physiological processes through redox-sensitive interactions. NXN interacts with myeloid differentiation primary response gene-88 (MYD88) and flightless-I (FLII) to regulate toll-like receptor 4 (TLR4)/MYD88 pathway activation, but FLII also regulates key cell processes and is secreted into the bloodstream. However, the effects of chronic ethanol consumption recapitulated by either ethanol alone or in combination with lipopolysaccharides (LPS), as a two-hit ALD model, on FLII/NXN/MYD88 complex and FLII secretion have not been explored yet. In this study, we have demonstrated that ethanol feeding increased FLII protein levels, its nuclear translocation and plasma secretion, and modified its tissue distribution in both *in vivo* and *in vitro* ALD models. Ethanol increased MYD88/FLII interaction ratio, and decreased NXN/MYD88 interaction ratio but this was partially reverted by two-hit model. While ethanol and two-hit model increased MYD88/TLR4 interaction ratio, two-hit model significantly decreased FLII nuclear translocation and its plasma secretion. Ethanol and LPS provoked similar effects *in vitro*; however, NXN overexpression partially reverted these alterations, and ethanol alone increased FLII secretion into culture medium. In summary, by analyzing the response of

[*]Corresponding author: Jaime Arellanes-Robledo; INMEGEN. Periférico Sur # 4809, Arenal Tepepan, Tlalpan, 14610. CDMX; Mexico. Phone: +5255 5350 1900; Ext. 1218. jarellanes@inmegen.gob.mx.

[§]Retired.

Conflict of interest

Authors have no conflict of interest.

FLII/NXN/MYD88 complex during ALD early progression both *in vivo* and *in vitro*, we have discovered that the effects of chronic ethanol consumption disrupt this complex and identified FLII as a candidate non-invasive plasma biomarker for the early detection of ALD.

Keywords

Alcohol consumption; Liver disease diagnosis; Non-invasive biomarkers; Nucleoredoxin; Oxidative stress

Introduction

Excessive alcohol consumption is a worldwide healthcare problem accounting for three million deaths in 2016 [1]. Development of alcoholic liver disease (ALD) may be attributed to multiple hits driving liver alterations by the synergistic effect of chronic alcohol consumption along with other risk factors that synergistically induce a number of liver injuries including steatosis, steatohepatitis, fibrosis, cirrhosis, hepatocellular carcinoma and associated complications [2]. ALD is closely linked to oxidative stress induction which is considered the primary mechanism of liver injury. In ALD, oxidative stress is the primary hit caused mainly by the increase of alcohol dehydrogenase (ADH) and cytochrome P450 2E1 (CYP2E1) activities [3] leading to the accumulation of acetaldehyde, the first metabolite of ethanol oxidation. The second hit is the leaky gut causing the release of lipopolysaccharides (LPS) into bloodstream, another strong inducer of oxidative stress and inflammation in the liver [4].

Currently, the diagnosis of alcohol-related liver diseases is based on the history of alcohol abuse, clinical evidence of liver disease, determination of indirect and direct non-invasive biomarkers, and imaging modalities such as elastography based on magnetic resonance and ultrasound that are mainly useful for the diagnosis of liver fibrosis [5, 6]. Determination of indirect biomarkers includes the measurement of transaminases activity either independent or in combination with others molecules, which are called second generation panel tests such as FibroTest, Hepascore and FibrometerA. For example, FibroTest combines a panel of the following five biochemical markers, α−2 macroglobulin, apolipoprotein A1, haptoglobin, gamma-glutamyl transferase, and total bilirubin [5, 7]. Direct biomarkers include the products of matrix synthesis or its degradation and the enzymes involved in these processes [5]. However, while non-invasive tests lack sensitivity and specificity and have limited utility for establishing a specific diagnosis as well as the severity of liver damage, the imaging techniques lack sensitivity and specificity for detecting early fibrosis stages; moreover, they are not useful in determining inflammation and hepatocellular injury [6]. In recent years, omics approaches have identified different ALD markers such as proteins contained in circulating extracellular vesicles, microRNAs and long-noncoding RNAs in preclinical studies [8, 9]. However, liver biopsy is still the gold standard for the diagnosis of chronic liver diseases [5, 6]. Despite the central role of oxidative stress in chronic liver diseases, few efforts have been addressed to identify oxidative stress-associated biomarkers in ALD progression.

Endogenous antioxidant molecules sense and balance intracellular oxidative stress but they may also function as intermediary signaling regulators [10]. Nucleoredoxin (NXN), an antioxidant enzyme, regulates several physiological processes through redox-sensitive interactions [11]. NXN interacts with myeloid differentiation primary response gene-88 (MYD88) and flightless-I (FLII) to regulate toll-like receptor 4 (TLR4)/MYD88 signaling pathway-dependent activation such as immunity and inflammation [12]. Additionally to its role in TLR4/MYD88 pathway, FLII is both an actin-remodeling protein and a nuclear receptor co-activator playing a vital function in cellular motility, contraction and adhesion, inflammation, wound healing and indirectly regulates collagen type-I expression [13–15]. FLII is also secreted *in vitro* by fibroblasts and macrophages, and it has been found in the human plasma. While fibroblasts increase FLII secretion when stressed by scratch wounding, macrophages temporally increase FLII secretion following LPS stimulus [16].

Moreover, recently it has been reported that NXN also interacts with FLII/Actin complex and it is altered during ALD progression [17]. Together, these data demonstrate that molecules that are involved in the regulation of increased oxidative stress might be specifically secreted into the blood stream directly in response to the early onset of ALD; therefore, their detection in the bloodstream might prove to be a viable non-invasive tool that contributes to the early diagnosis and monitoring of ALD progression.

The aim of this investigation was to analyze FLII/NXN/MYD88 complex and FLII status in response to the effects of chronic ethanol consumption in the mouse liver as well as to ethanol exposition in an *in vitro* system. The role of NXN overexpression on ethanol effects was also determined *in vitro*. We demonstrated that ethanol disrupts the complex and increases FLII secretion both *in vivo* and *in vitro*.

Materials and Methods

Alcoholic liver disease mouse model

Animals received proper care in accordance with the Institutional Animal Use and Care Committee of the Veteran Affairs Medical Center and of The George Washington University (Washington, D.C., USA). Animals were subjected to the high-fat Lieber-DeCarli liquid diet regime plus single-binge of ethanol to induce the early stage of ALD, as previously described [18]. Briefly, after a gradual ramp-up period, six-week-old female wild-type C57BL/6 mice (body wt ~20g, n=5 per group) were subjected to 5% ethanol in liquid diet for 4 weeks. Control group (**C**) was pair-fed with a isocaloric diet; Ethanol/Binge group (**E**) was fed with 5% (w/v) ethanol diet for 4 weeks and then it received a single oral dose of 3.2 g ethanol per kg body weight (stock solution of 32% w/v ethanol in saline buffer). Ethanol/Binge/LPS group (**EL**) was treated similarly as the Ethanol/Binge group, but in addition, each animal received a single dose of LPS (2 mg/kg, i.p.). This LPS dose was selected based upon previous investigations where the acute LPS effects, as a second hit, on ALD models were evaluated [19]. Mice were euthanized six hours after ethanol and/or LPS administration. Euthanasia was performed by exsanguination under isoflurane anesthesia; immediately, plasma was separated from the blood and pieces of the dissected liver were split for total, cytosolic and nuclear protein extracts, and for confocal microscopy. All collected samples were stored at −75°C for further analyses.

Co-culture model

Hepatic stellate cells (HSC) and VL17A cells were co-cultured as previously described [18]. HSC were isolated from human livers obtained during gastric bypass surgery for morbid obesity by the pronase-collagenase method previously described [20]. VL17A cells were a courtesy of Dr. Dahn L. Clemens from the Liver Study Unit, VA Medical Center, Omaha; Nebraska. VL17A cells are HepG2 cells that constitutively express both CYP2E1 and ADH enzymes [21]. Co-cultures of HSC/VL17A cells were cultured in ratio of 1:10 to closely mimic the *in vivo* conditions in whole liver [22]. Co-cultures were grown to semi-confluence in regular culture medium containing dulbecco's modified Eagle's medium F12 (DMEM-F12, from ATCC; Manassas, VA), 10% (v/v) fetal bovine serum (FBS), 1% (v/v) penicillin/streptomycin, 5 mg/l ITS and dexamethasone 10^{-7} M. Eighteen hours before ethanol exposure, culture medium was replaced for DMEM-F12reduced FBS (0.1%, v/v) medium to synchronize cells activity and then cells were subjected to different treatments indicated below.

Nucleoredoxin transfection and ethanol treatment *in vitro*

Nucleoredoxin transfection and ethanol treatments were performed as previously described [18]. Briefly, co-cultures were transfected with 1 μg/ml of NXN plasmid or empty vector (EV) (A friendly courtesy of Drs. Funato and Miki from the Institute of Medical Science, University of Tokyo, Japan) for 24 h using Lipofectamine LTX & Plus Reagent kit in OPTI-MEM medium (Life Technologies; Grand Island, NY) according to the manufacturer instructions; then, OPTI-MEM medium was replaced by DMEM-F12-reduced FBS medium. Co-cultures transfected with EV were called untransfected cells. After 18 h, ethanol was added at 100 mM final concentration for 48 h. Then, both untransfected and transfected co-cultures were treated with LPS (1 μg/ml) and incubated for 3 h. Untransfected cells were exposed to different treatments as follows: untreated control (**C**), ethanol (**E**), LPS (**L**) and ethanol plus LPS (**EL**). Similar groups were included for NXN-transfected cells which were indicated as **N**, **NE**, **NL**, and **NEL**, respectively. To prevent death by the prolonged period of starvation time of co-cultures exposed to ethanol for one week, ethanol was mixed in regular culture medium and the mix was daily replaced. For all *in vitro* determinations three independent experiments were carried out in duplicated (n=6 per group).

Protein extraction from liver tissues, co-cultures, and culture media

Total protein extracts were prepared as previously reported [14]. Briefly, lysis buffer contained 50 mM Tris (pH 8), 150 mM NaCl, 200 mM EDTA, 100 mM NaF, 10 mM sodium pyrophosphate, 2 mM Na3VO4, 1 mM phenylmethylsulfonyl fluoride, 0.5% (v/v) NP-40, (All from Sigma; St. Louis, MO), Complete and PhosSTOP (Roche, Branchburg, NJ). Lysates were incubated on rocking for 30 min, centrifuged at 16000 g for 10 min at 4°C and stored at –75°C for further analyses. Cytosolic and nuclear protein from mice liver and cell co-cultures were extracted as previously described with some modifications [24]. While frozen hepatic tissues (~100 mg) were first homogenized in 1.0 ml of ice-cold lysis buffer A [10 mM HEPES, pH 7.9, 10 mM KCl, 0.1 mM EDTA, 0.1 mM EGTA (All from Sigma; St. Louis, MO), Complete and PhoSTOP (Roche, Branchburg, NJ)], cells were washed once with ice-cold PBS and then lysed in 0.5 ml of the same buffer A. Lysed samples were

incubated on ice for 15 min with occasional mixing. Then, 30 μl of 10% NP-40 solution was added; vortexed vigorously for 15 sec, centrifuged at 16000 g for 30 sec and supernatant was stored at –75°C as the cytosolic protein fraction. Pellets containing intact nuclei were washed twice in buffer A, resuspended in ice-cold buffer B [20 mM HEPES, pH 7.9, 0.4 mM NaCl, 1 mM EDTA, 1 mM EGTA, 0.6% NP-40 (All from Sigma; St. Louis, MO), Complete and PhoSTOP (Roche, Branchburg, NJ)], rocked in a shaking platform for 15 min at 4°C, centrifuged in a micro-centrifuge for 30 min at 16,000 g and supernatant was stored at –75°C as the nuclear protein fraction for further analyses. To determine FLII presence in culture media, after treatment times, media were quickly collected and supplied with Complete (Roche). Then culture media were centrifuged at 1200 *g* for 10 min at 4°C, separated in a clean tube and centrifuged again at 16000 *g* for 10 min at 4°C. Supernatants were prepared for western blot analysis. All procedures were performed at 4°C to reduce protein degradation.

Western blot analysis

Equivalent amounts of boiled protein in Laemmli's buffer were analyzed through SDS-PAGE and transferred to a PVDF membrane. Antibodies against NXN (GTX107039) and ADH1 (GTX62515) were from GeneTex Inc (Irvine, CA); CYP2E1 (ab28146) was from Abcam (Cambridge, MA); FLII (muse-116.40, sc21716), MYD88 (goat-N19, sc8196; and mouse-E11, sc74532), TLR4 (25, sc-293072), and Lamin B (M20, sc-6217) were from Santa Cruz biotechnology (Santa Cruz, CA); Caspase-3 (9662) was from Cell Signaling Technology (Danvers, MA); and β-actin (A5441) was from Sigma (St. Louis, MO). Protein loading was confirmed by reprobing of the blots with anti-β-actin or anti-Lamin B for cytosolic and nuclear fractions, respectively. Densitometric analyses were carried out using ImageJ software (NIH). Densitometric data from Coomassie Blue-stained gels were used as loading controls to normalize protein levels detected in culture media.

Immunoprecipitation (IP) assay

Proteins extracted either from liver tissues or cell co-cultures were solubilized with the ice-cold lysis buffer containing 20 mM Tris-Cl, pH 7.8, 137 mM NaCl, 1% (v/v) Nonidet P40, 10% (v/v) glycerol, 2 mM EDTA (All from Sigma; St. Louis, MO), supplied with Complete and PhoSTOP (Roche, Branchburg, NJ) as previously described [23]. FLII and MYD88 proteins were immunoprecitated with protein A/G Plus-Agarose beads (sc2003, Santa Cruz Biotechnol.) in complex with either anti-FLII (rabbit-H300, sc30046) or anti-MYD88 (mouse-E11, sc74532) antibodies, respectively. After IP assays, FLII and MYD88 protein were immunodetected by western blot analyses with anti-FLII (muse-116.40, sc21716) and anti-MYD88 (goat-N19, sc8196) antibodies, respectively; while NXN and TLR4 were immunodetected using anti-NXN (GTX107039) and anti-TLR4 (25, sc-293072). Co-precipitated were normalized by reprobing the blots to detect the constant regions (heavy chains) of the immunoglobulins used for IP assays, as previously indicated [24].

Immunofluorescence (IF) staining

Five micrometers-thick fresh-frozen liver sections were rinsed twice in ice-cold PBS, fixed with 4% formaldehyde in PBS (pH 7.4) for 10 min at room temperature, washed three times and incubated for 1 h with washing solution [0.25% Triton X-100 in PBS (PBST)].

Then, sections were blocked with 1% BSA in PBST for 30 min at room temperature and incubated with anti-FLII antibody (rabbit-H300, sc30046, 1:300) overnight at 4°C in blocking solution. Then, sections were washed three times followed by Alexa Fluor 488 donkey anti-rabbit 1:500 (Life technologies) and incubated for 1 h at room temperature in the dark. Actin cytoskeleton and nuclear DNA were stained with Alexa Fluor 568 Phalloidin (1:1000) and ToPro (1:500) (Life technologies) for 30 min at room temperature, respectively. Finally, sections were rinsed, drained and fixed using Prolong Gold antifade reagent (Life Technologies, Grand Island, NY). Pictures were captured using Zeiss LSM 710 Axio Observer confocal microscopy.

Enzyme-linked immunosorbent assay (ELISA) for FLII quantification in mice plasma

High-binding 96 ELISA plates were coated with mouse anti-FLII antibody (Santa Cruz Biotechnol, sc-21716) at 2 μg/ml final concentration diluted in binding buffer (150 mM Na_2CO_3, 350 mM $NaHCO_3$, pH 9.6), covered, sealed and incubated overnight at 4°C. Then plates were washed and blocked with 1% BSA in TBS buffer for 2 h at room temperature. After washing, 50 μl of plasma samples (1:10 in blocking buffer) were added and incubated at 37°C for 2 h. Then, rabbit anti-FLII (Santa Cruz Biotechnol, sc30046) diluted 1:100 in blocking buffer was added and incubated overnight at 4°C. Finally, chicken anti-rabbit IgG-HRP (sc-2963, 1:2000) was added, incubated for 2 h at room temperature, washed and then peroxidase activity was detected using TMB peroxisase substrate kit (Vector Labs. Burlingame, CA); finally, the signal was measured at 650 nm.

Statistical analyses

Statistical analyses were performed using GraphPad Prism 7.0 software. Data calculations were performed using one-way ANOVA followed by Bonferroni's post-hoc test. For *in vivo* experiments five animals per group were included, while for *in vitro* experiments three independent experiments were carried out in duplicated (six per group). Data are expressed as mean ±SE. Differences were considered significant when $p<0.05$.

Results

Ethanol disrupts FLII/NXN/MYD88 complex and increases FLII levels

We first investigated the effects of ethanol and two-hit model on FLII/NXN/MYD88 complex. IP analysis of MYD88 revealed that NXN/MYD88 interaction ratio was decreased 56% ($p<0.001$) and 40% ($p=0.004$) by ethanol and by two-hit model, respectively, showing that two-hit partially restored the binding ratio as compared to ethanol alone (Figure 1A). Conversely, both ethanol and two-hit model induced 2.3 ($p=0.008$) and 2.8 ($p<0.001$) fold the MYD88/TLR4 interaction ratio, respectively. Although FLII was co-precipitated 1.5 ($p=0.03$) fold higher in ethanol, MYD88 level was increased 1.4 ($p=0.02$) fold by two-hit model as compared to controls (Figure 1A). On the other hand, FLII IP analysis showed that FLII/NXN/MYD88 interaction ratio was not significantly altered; however, anti-FLII antibody precipitated 1.4 ($p=0.008$) fold FLII levels in ethanol group as compared to controls. This increment was reverted by two-hit model (Figure 1B). To investigate the effects of ethanol on FLII compartmentalization, we then evaluated its cytosolic and nuclear status in mice liver. As shown in Figure 1C, ethanol increased 1.2 ($p=0.02$) and 1.4

(p=0.004) fold the cytosolic and nuclear FLII content, respectively; contrastingly, two-hit model decreased more than 20% (p=0.03) and 44% (p<0.001) FLII nuclear translocation as compared to control and ethanol groups, respectively.

Ethanol alters FLII distribution in liver tissue and increases its secretion into the plasma

To determine the structural localization of FLII, we carried out IF analysis in mice liver tissues. The analysis revealed that FLII was homogeneously distributed within the whole liver structure accompanied by a well-organized structure of actin filaments in control tissues (Figure 2). Interestingly, FLII signal was mostly localized surrounding the central veins of liver tissues treated with ethanol; however, this arrangement became diffusely redistributed throughout the whole liver tissue by two-hit model. Additionally, actin filaments were partially disarranged by this treatment. On the other hand, our investigation on the effect of ethanol on FLII secretion into mice bloodstream as determined by IP (Figure 3A) and ELISA (Figure 3B) analyses, revealed that ethanol increased the secretion of FLII into the plasma more than 1.8 (p=0.03) and 1.5 (p<0.001) fold, respectively; but this increment was disrupted by two-hit model.

FLII/NXN/MYD88 interaction ratio and FLII status are altered by ethanol but partially reverted by NXN overexpression *in vitro*

To explore the effects of ethanol and/or LPS on FLII/NXN/MYD88 complex *in vitro*, we used a co-culture model of liver cells consisting of human HSC and VL17A hepatocytes-like cells. As expected, while basal levels were detected in untransfected cells, NXN was co-precipitated more than 3 (p<0.001) fold in NXN-transfected cells (Figure 4A & 4B). No significant changes were observed on NXN/MYD88 interaction ratio in untransfected cells; however, LPS decreased 15% (p=0.002) the interaction ratio in NXN overexpressing cells. While MYD88/TLR4 complex ratio was unaltered in untransfected cells, LPS increased 1.4 fold (p<0.001) this binding ratio in NXN-transfected cells (Figure 4A & 4C); all of them as compared to their respective controls. As shown in Figure 4A & 4D, ethanol and LPS alone increased 1.3 (p=0.01) and 2.0 (p<0.001) fold, respectively, the binding ratio of MYD88/FLII complex. This increment was not observed by their combined effects Interestingly, NXN transfection by itself promoted this binding ratio by 1.7 (p<0.001) fold compared to untransfected control cells. Although neither ethanol nor LPS alone altered this condition, their combination disrupted it similar than in untransfected cells. IP assay revealed that MYD88 levels were not affected by either different treatments or NXN transfection (Figure 4A & 4E). IP of FLII revealed that while ethanol and LPS alone increased 1.3 (p<0.001) fold its binding ratio with NXN, their combination reverted this increment in untransfected cells (Figure 5A & 5B). This increment was slight but significantly induced (1.2 fold, p<0.01) by LPS in NXN-transfected cells as compared to their respective controls. Ethanol and LPS alone, and their combination increased 1.3 (p=0.03), 1.9 (p<0.001) and 1.3 (p=0.03) fold, respectively, the co-precipitation of TLR4 in untranfected cells (Figure 5A & 5C). This increment was not observed in NXN overexpressing cells as compared to NXN-transfected controls, but it was significantly higher (more than 1.6 fold, p<0.001) as compared to untransfected controls. FLII protein levels were increased more than 1.5 and 2.2 (p<0.001) fold by LPS and by ethanol plus LPS, respectively, in untransfected cells as compared to controls (Figure 5A & 5D); however, this increment was not observed in

NXN-transfected cells. Contrary, FLII levels were decreased 38% (p=0.002) by ethanol in combination with LPS in NXN overexpressing cells as compared to NXN-transfected controls. Finally, increased levels of MYD88 (1.3 fold, p=0.004) were observed in NXN-transfected controls as compared to untransfected controls (Figure 5A & 5E).

Our results on FLII status (Figure 6A) showed that FLII levels were increased more than 1.2 (p<0.001) fold by the combination of ethanol plus LPS in untrasfected co-cultures, but this increment was reverted 15 (p=0.01), 16 (p=0.004) and 28% (p<0.001) by NXN overexpression in ethanol, LPS and their combination, respectively, as compared to NXN-transfected controls. This decrement was higher (23, 25 and 42% respectively, p<0.001) when compared to the same treatments in untransfected cells. Then, cytosolic and nuclear contents of FLI were evaluated. Similar than in total protein, NXN overexpression diminished 16 (p=0.03), 21 (p=0.002) and 34% (p<0.001) the cytosolic levels of FLII either in ethanol and LPS alone or their combination, respectively (Figure 6B). While FLII nuclear translocation was increased 1.3 (p=0.04), 1.5 (p<0.001) and 1.7 (p<0.001) fold by ethanol and LPS alone or their combination, respectively, in untransfected cells as compared to unstransfected controls, this translocation was decreased 29% (p=0.007), 31 (p=0.004) and 39% (p<0.001) by NXN overexpression in ethanol and LPS alone as well as by their combination, respectively, as compared to NXN-transfected controls (Figure 6C).

Ethanol increases FLII secretion into cell culture media

As shown in Figure 7A, ethanol induced the secretion of FLII into culture media more than 1.7 (p=0.001) fold at 24 h; interestingly, this secretion increased more than 3 (p<0.001) fold at 48 h in both untransfected and NXN-transfected co-cultures but FLII secretion was unaffected by LPS alone irrespective of NXN expression (Figure 7B). To discard that presence of FLII was because of cells breaking, the presence of β-Actin was also detected in cultures media collected at 24 and 48 h (Fig. 7A & 7B); additionally, apoptosis was also discarded by detecting Procaspase-3 cleavage in total protein from co-cultures exposed to ethanol and/or LPS for 48 h. Neither β-Actin in culture media nor cleaved Caspase-3 in co-culture total protein were detected (Fig. 7C). To investigate whether FLII secretion is persistent for a longer period of time to ethanol exposition, untransfected co-cultures were exposed to ethanol for up to one week. Fresh culture media containing ethanol, were replaced every 24 h for seven days and in the last day culture media were collected. Figure 8A shows that even after seven days of ethanol exposition, co-cultures still secreted high levels of FLII into the culture media (2.4 fold, p<0.001) as compared to unexposed co-cultures. We also investigated whether ethanol effects increased FLII secretion because of cells breaking by detecting the presence of β-Actin in culture media after seven days of ethanol exposition. The presence of β-Actin was not detected in culture media (Figure 8A). Finally, we also determined CYP2E1, ADH1 and FLII levels in total protein extracted from co-cultures after seven days of ethanol exposition. As shown in Figure 8B, their protein levels were still increased, confirming that ethanol-metabolizing enzymes as well as FLII protein were still increased by ethanol effects.

Discussion

The causative role of oxidative stress on ALD pathogenesis has been widely documented [25]. Excessive alcohol consumption augments reactive oxygen species (ROS) production, activates NADPH oxidase complex in hepatocytes, leading to an increased production of superoxide, induces mitochondrial dysfunction, and depletes endogenous antioxidants defense system [25]. Protection from these alterations by exogenous antioxidant compounds and genetic manipulation of antioxidant genes has confirmed these facts. The capability to promote oxidative injury by ethanol has encouraged studies seeking for biomarkers directly associated to oxidative stress such as lipid peroxidation products, oxidative DNA modifications and protein adducts [26]. Nevertheless, little attention has been paid to molecules that might respond to oxidative stress promoted by excessive ethanol consumption. Here, we determined the effect of ethanol on the redox-sensitive FLII/NXN/MYD88 complex in a well-characterized ALD *in vivo* model that uses female as the most susceptible gender of mice [27–29] and in an *in vitro* system [18].

As a redox sensor enzyme, NXN interacts with several molecules in a redox-dependent manner to negatively regulate physiological processes. When oxidative stress imbalances the physiologic redox status, NXN becomes oxidized leading to its dissociation from the molecular complexes and as a result, it may facilitate the downstream functions [11]. e.g. oxidative stress produced by either acetaldehyde, the first metabolite of ethanol oxidation, or the combination of ethanol plus LPS, imbalances NXN/DVL interaction ratio and increases fibrogenic genes expression as well as phosphoinositides production, respectively, both of which involve DVL participation [18, 23]. Based on the oxidative stress increment induced by our ALD models as well as on these key evidences, we now propose that FLII/NXN/MYD88 complex might also be a target of both ethanol and LPS. LPS. This complex is involved in TLR4/MYD88 signaling pathway regulation. Upon LPS stimulation, TLR4 induces the recruitment of MyD88 to TLR4, which leads to the nuclear translocation of NF-κB to turn on genes transcription involved in innate immunity and inflammation which could be also altered as a result of chronic ethanol consumption. In this scenario, to prevent the unnecessary TLR4/MYD88 pathway hyperactivation, FLII binds to MYD88 through NXN. The central protective role of NXN in this complex mechanism relies on the fact that upon its inactivation; the pathway remains hyperactivated because the sequestering of MYD88 from TLR4 by FLII is not performed [12]. Thus, the participation of FLII/NXN/MYD88 complex in ALD progression could be preferentially linked to LPS stimuli. This is because it is well-known that excessive ethanol consumption promotes LPS translocation from the gut into the bloodstream. Upon reaching the liver, LPS activates TLR4 on HSC and Kupffer cells, thereby increasing ROS production which in turn, potentiates the liver damage, a phenomenon known as endotoxemia that may occur early during ALD pathogenesis [25, 30]. Herein, using a well-known *in vivo* model that recapitulate steatosis, an early ALD alteration, but not more severe forms such as fibrosis [31], we showed that ethanol feeding resulted in a decrement of NXN/MYD88 interaction ratio, but increased MYD88/FLII and MYD88/TLR4 ratios. Surprisingly, two-hit model partially reverted ethanol-disrupted NXN/MYD88 ratio (Fig. 1). Ethanol and LPS treatments provoked similar alterations on FLII/NXN/MYD88 complex in co-cultures; however, these disruptions were

partially reverted by NXN overexpression (Fig. 5 & 6). Based on previous findings showing that these *in vivo* and *in vitro* models exhibit increased oxidative stress in response to ethanol and/or LPS, and on the fact that low doses of LPS attenuated mice liver injury induced by diethylnitrosamine as well as reverted the altered NXN/DVL interaction ratio as a phenomenon called hepatic tolerance [18, 32], our results indicate that the reversal effect of two-hit model on FLII/NXN/MYD88 complex might be due to the development of hepatic tolerance provoked by LPS and then NXN is required to regulate additional molecular events; as a result, NXN prioritizes its interaction with MYD88 to neutralize the hyperactivation of TLR4/MYD88 signaling pathway which could have been promoted by the cumulative stress induced by LPS administration. Although in an oxidative environment NXN decreases its redox-sensitive interaction ratios by becoming oxidized, its response to LPS stimulus suggests that even under that condition NXN may be functional to regulate TLR4/MYD88-dependent activity, a mechanism that needs to be clarified by determining its downstream response to ethanol effects. Altogether, these findings indicate that disruption of FLII/NXN/MYD88 complex by ethanol is an early ALD molecular alteration promoted by the primary mechanism of liver injury, oxidative stress; and at this point, NXN is still active to regulate the adverse effects promoted by ethanol and/or LPS. This conclusion is in part supported by the protective activity played by NXN overexpression on FLII/NXN/MYD88 complex integrity.

In addition to participate in several physiological functions such as cellular motility, contraction and adhesion, inflammation, wound healing, among others [13–15], it has been shown that under stressed conditions FLII is secreted into both cell culture and plasma [33]. Thus, the analysis of FLII/NXN/MYD88 complex led us to investigate the FLII status in terms of cytosolic and nuclear compartmentalization, liver structural localization and secretion during ALD early progression. Our results showed that while ethanol alone increased both cytosolic and nuclear FLII content, and induced its accumulation surrounding the central veins of liver tissues, two-hit model reverted these effects and partially disarranged actin filaments (Figs. 1 & 2). Interestingly, *in vitro* results showed that ethanol, LPS or their combination, increased the nuclear but not the cytosolic content of FLII. This phenomenon was reverted by NXN overexpression (Fig. 4). Similar to FLII compartmentalization analysis, ethanol but not two-hit model increased FLII secretion into mice plasma (Fig. 3); coincidentally, ethanol but not LPS also increased FLII secretion into the culture media; however, NXN overexpression did not modify this condition. Of note, FLII was actively secreted even after one week of ethanol exposure *in vitro* (Figs. 7 & 8). In this regard, since we have recently reported that FLII nuclear compartmentalization was altered by the combined effect of ethanol, LPS and the liver carcinogen diethylnitrosamine (DEN) after ten weeks of ethanol and DEN, and five weeks of LPS administration [17], it is plausible to propose that FLII secretion might be an altered process even at later ALD sages; a phenomenon that need to be clarified. Together, these data show that although some similarities were found, results may well be entirely different when *in vivo vs in vitro* experiments are compared; specially, because of the implicit complexity of the *in vivo* systemic response that is absent in cell cultures, among others variables. This can explain why ethanol plus LPS induced FLII nuclear translocation in co-cultures but not in animals subjected to the same hepatotoxins (Figs. 1 & 4).

FLII levels increase in response to tissue injury similar to its increased secretion in scratch wounding. Secreted FLII binds to LPS and as a result, inhibits macrophage-dependent inflammation. While its increment reduces cell migration, impairs wound healing and increases scar formation, low levels of FLII accelerate wound healing [14, 16, 34]. Thus, it has been proposed that increased FLII in wounds might be a mechanism to inhibit inflammation by binding to LPS and negatively regulate the activation of TLR signaling [16]. Several evidences have shown that combination of high-fat diet with chronic ethanol consumption impairs wound healing [35]. A recent investigation has shown that such a combination of dietary intake decreases skin wound healing, a phenomenon closely linked to an increased inflammation as well as oxidative stress [36]. It has been well characterized that ALD models based on high-fat diet plus either chronic or acute ethanol feeding capitulate the early stages of the disease by inducing steatosis, inflammation, ALT and AST liver injury markers [31, 37, 38]. Similarly, LPS-dependent endotoxemia has been associated with the early pathogenesis of ALD [30]. Using a similar ALD model, we went one step further by investigation FLII secretion status that along with those already described could strengthen the prognosis of the early ALD progression. Thus, here we have demonstrated that FLII secretion was increased by ethanol feeding but not by ethanol plus LPS (Fig. 3). This increment was also recapitulated *in vitro*, but LPS administration did not modify the levels of secreted FLII induced by ethanol alone (Fig. 7 & 8). Altogether, these data indicate that increased FLII secretion into bloodstream may be an early viable marker for the onset of ALD progression, and strongly suggest that its increased secretion might be an attempt to suppress liver inflammation induced by chronic ethanol exposure.

Currently, liver biopsy is still the gold standard for the diagnosis of chronic liver diseases. Although some others imaging technics such as magnetic resonance and ultrasound elastographies have been developed, these technics lack sensitivity and specificity for the detection of early stages of chronic liver diseases; furthermore, they are not useful for determining inflammation and hepatocellular injury [6]. Additionally, indirect biomarkers such as ALT and AST have been the mainstay for clinical decisions on chronic liver disease management; however, they show inaccurate prognostic value, e.g. they were not able to predict the liver fibrosis stage based on N-terminal type III collagen propeptide determination [39]. Therefore, novel approaches that can fill these gaps might provide significant advances for the diagnosis and monitoring of ALD progression at the clinical level [6]. Thus, identification of molecules directly targeted by ethanol and secreted into the bloodstream may indeed prove to be a viable specific and sensitive clinical markers for the early identification of ALD and its progression.

However, in the efforts for identifying biomarkers that specifically predict the stage of a disease, it is very risky to believe that a single molecule can meet that requirement. Here we showed that secretion of FLII into bloodstream is increased by ethanol as an early liver alteration. Thus, we now propose that plasma FLII in combination with a battery of other viable biomarkers might prove to be a more effective set of biomarkers rather than a single biomarker to identify ALD at an early stage. This result supports the further evaluation of FLII in a clinical trial.

In summary, by investigating the effects of ethanol either alone or in combination with LPS on FLII/NXN/MYD88 complex, we have identified FLII as a potential plasma biomarker of ALD. This is based on a mechanism that involves the disruption of FLII/NXN/MYD88 complex and the increment of FLII levels and secretion into the blood circulation in response to the effects of chronic ethanol consumption. We have also demonstrated that while ethanol alone disrupts the complex and increases FLII secretion, ethanol plus LPS partially reverts these conditions (Fig. 9). The reversal effect on FLII secretion by LPS may be due to the possible attempts by the liver cells to prevent ethanol-induced inflammation by neutralizing the hyperactivation of TLR4/MYD88 signaling pathway. Additionally, although FLII secretion was unaffected by either NXN overexpression or LPS administration *in vitro*, NXN overexpression has the capability to modify the response of FLII/NXN/MYD88 complex to ethanol and/or LPS effects.

Acknowledgments

This work was funded by the National Institute on Alcohol Abuse and Alcoholism grant RO1 AA010541 (MRL). JAR expresses his sincere thanks to Cátedras-CONACYT program. KRG, RS and JAR are deeply grateful for the invaluable support of Dr. Marcos Rojkind†. Authors express their gratitude to Dr. Dahn L. Clemens for providing VL17A cells (Liver Study Unit, VA Medical Center, Omaha; Nebraska) and Drs. Funato and Miki (Institute of Medical Science, University of Tokyo, Japan) for providing NXN plasmid.

Abbreviations

ALD	alcoholic liver disease
ALT	alanine aminotransaminase
AST	aspartate aminotransaminase
BSA	bovine serum albumin
C	control group
DEN	diethylnitrosamine
DMEM	dulbecco’s modified eagle’s medium
ELISA	enzyme-linked immunosorbent assay
E	ethanol/binge model
FBS	fetal bovine serum
HSC	hepatic stellate cells
ITS	insulin-transferrin-sodium selenite
LPS	lipopolysaccharide
PVDF	polyvinylidene difluoride

†Deceased.

ROS	reactive oxygen species
SDS-PAGE	sodium dodecyl sulfate polyacrylamide gel electrophoresis
TH	ethanol/binge/LPS “two-hit” model

References

[1]. World Health Organization (WHO). Global Status Report on Alcohol and Health. Geneva. Available at https://www.who.int/substance_abuse/publications/global_alcohol_report/en/ Accessed January 10, 2020., (2018).

[2]. Thursz M, Kamath PS, Mathurin P, Szabo G, Shah VH, Alcohol-related liver disease: Areas of consensus, unmet needs and opportunities for further study, Journal of hepatology 70(3) (2019) 521–530. [PubMed: 30658117]

[3]. Seitz HK, The role of cytochrome P4502E1 in the pathogenesis of alcoholic liver disease and carcinogenesis, Chem Biol Interact 316 (2019) 108918. [PubMed: 31836462]

[4]. Ceni E, Mello T, Galli A, Pathogenesis of alcoholic liver disease: role of oxidative metabolism, World J Gastroenterol 20(47) (2014) 17756–72. [PubMed: 25548474]

[5]. Chrostek L, Panasiuk A, Liver fibrosis markers in alcoholic liver disease, World J Gastroenterol 20(25) (2014) 8018–23. [PubMed: 25009372]

[6]. Mann J, Reeves HL, Feldstein AE, Liquid biopsy for liver diseases, Gut 67(12) (2018) 2204–2212. [PubMed: 30177542]

[7]. Imbert-Bismut F, Ratziu V, Pieroni L, Charlotte F, Benhamou Y, Poynard T, Group M, Biochemical markers of liver fibrosis in patients with hepatitis C virus infection: a prospective study, Lancet 357(9262) (2001) 1069–75. [PubMed: 11297957]

[8]. Shabangu CS, Huang JF, Hsiao HH, Yu ML, Chuang WL, Wang SC, Liquid Biopsy for the Diagnosis of Viral Hepatitis, Fatty Liver Steatosis, and Alcoholic Liver Diseases, Int J Mol Sci 21(10) (2020).

[9]. Hadefi A, Degre D, Trepo E, Moreno C, Noninvasive diagnosis in alcohol-related liver disease, Health Sci Rep 3(1) (2020) e146. [PubMed: 32166191]

[10]. Fujino G, Noguchi T, Takeda K, Ichijo H, Thioredoxin and protein kinases in redox signaling, Seminars in cancer biology 16(6) (2006) 427–35. [PubMed: 17081769]

[11]. Funato Y, Miki H, Nucleoredoxin, a novel thioredoxin family member involved in cell growth and differentiation, Antioxidants & redox signaling 9(8) (2007) 1035–57. [PubMed: 17567240]

[12]. Hayashi T, Funato Y, Terabayashi T, Morinaka A, Sakamoto R, Ichise H, Fukuda H, Yoshida N, Miki H, Nucleoredoxin negatively regulates Toll-like receptor 4 signaling via recruitment of flightless-I to myeloid differentiation primary response gene (88), J Biol Chem 285(24) (2010) 18586–93. [PubMed: 20400501]

[13]. Kopecki Z, Cowin AJ, Flightless I: an actin-remodelling protein and an important negative regulator of wound repair, Int J Biochem Cell Biol 40(8) (2008) 1415–9. [PubMed: 17526423]

[14]. Cowin AJ, Adams DH, Strudwick XL, Chan H, Hooper JA, Sander GR, Rayner TE, Matthaei KI, Powell BC, Campbell HD, Flightless I deficiency enhances wound repair by increasing cell migration and proliferation, J Pathol 211(5) (2007) 572–81. [PubMed: 17326236]

[15]. Li J, Yin HL, Yuan J, Flightless-I regulates proinflammatory caspases by selectively modulating intracellular localization and caspase activity, The Journal of cell biology 181(2) (2008) 321–33. [PubMed: 18411310]

[16]. Lei N, Franken L, Ruzehaji N, Offenhauser C, Cowin AJ, Murray RZ, Flightless, secreted through a late endosome/lysosome pathway, binds LPS and dampens cytokine secretion, J Cell Sci 125(Pt 18) (2012) 4288–96. [PubMed: 22718342]

[17]. Alarcon-Sanchez BR, Guerrero-Escalera D, Rosas-Madrigal S, Ivette Aparicio-Bautista D, Reyes-Gordillo K, Lakshman MR, Ortiz-Fernandez A, Quezada H, Medina-Contreras O, Villa-Trevino S, Isael Perez-Carreon J, Arellanes-Robledo J, Nucleoredoxin interaction with flightless-I/actin complex is differentially altered in alcoholic liver disease, Basic Clin Pharmacol Toxicol (2020).

[18]. Arellanes-Robledo J, Reyes-Gordillo K, Ibrahim J, Leckey L, Shah R, Lakshman MR, Ethanol targets nucleoredoxin/dishevelled interactions and stimulates phosphatidylinositol 4-phosphate production in vivo and in vitro, Biochem Pharmacol 156 (2018) 135–146. [PubMed: 30125555]

[19]. Schaffert CS, Duryee MJ, Hunter CD, Hamilton BC 3rd, DeVeney AL, Huerter MM, Klassen LW, Thiele GM, Alcohol metabolites and lipopolysaccharide: roles in the development and/or progression of alcoholic liver disease, World J Gastroenterol 15(10) (2009) 1209–18. [PubMed: 19291821]

[20]. Svegliati-Baroni G, Ridolfi F, Di Sario A, Saccomanno S, Bendia E, Benedetti A, Greenwel P, Intracellular signaling pathways involved in acetaldehyde-induced collagen and fibronectin gene expression in human hepatic stellate cells, Hepatology 33(5) (2001) 1130–40. [PubMed: 11343241]

[21]. Donohue TM, Osna NA, Clemens DL, Recombinant Hep G2 cells that express alcohol dehydrogenase and cytochrome P450 2E1 as a model of ethanol-elicited cytotoxicity, Int J Biochem Cell Biol 38(1) (2006) 92–101. [PubMed: 16181800]

[22]. Geerts A, History, heterogeneity, developmental biology, and functions of quiescent hepatic stellate cells, Seminars in liver disease 21(3) (2001) 311–35. [PubMed: 11586463]

[23]. Arellanes-Robledo J, Reyes-Gordillo K, Shah R, Dominguez-Rosales JA, Hernandez-Nazara ZH, Ramirez F, Rojkind M, Lakshman MR, Fibrogenic actions of acetaldehyde are beta-catenin dependent but Wingless independent: a critical role of nucleoredoxin and reactive oxygen species in human hepatic stellate cells, Free radical biology & medicine 65 (2013) 1487–96. [PubMed: 23880292]

[24]. Rogstad SM, Sorkina T, Sorkin A, Wu CC, Improved precision of proteomic measurements in immunoprecipitation based purifications using relative quantitation, Anal Chem 85(9) (2013) 4301–6. [PubMed: 23517085]

[25]. Sid B, Verrax J, Calderon PB, Role of oxidative stress in the pathogenesis of alcohol-induced liver disease, Free Radic Res 47(11) (2013) 894–904. [PubMed: 23800214]

[26]. Zhu H, Jia Z, Misra H, Li YR, Oxidative stress and redox signaling mechanisms of alcoholic liver disease: updated experimental and clinical evidence, Journal of digestive diseases 13(3) (2012) 133–42. [PubMed: 22356308]

[27]. Bertola A, Mathews S, Ki SH, Wang H, Gao B, Mouse model of chronic and binge ethanol feeding (the NIAAA model), Nat Protoc 8(3) (2013) 627–37. [PubMed: 23449255]

[28]. Li SQ, Wang P, Wang DM, Lu HJ, Li RF, Duan LX, Zhu S, Wang SL, Zhang YY, Wang YL, Molecular mechanism for the influence of gender dimorphism on alcoholic liver injury in mice, Hum Exp Toxicol 38(1) (2019) 65–81. [PubMed: 29792338]

[29]. Kono H, Wheeler MD, Rusyn I, Lin M, Seabra V, Rivera CA, Bradford BU, Forman DT, Thurman RG, Gender differences in early alcohol-induced liver injury: role of CD14, NF-kappaB, and TNF-alpha, Am J Physiol Gastrointest Liver Physiol 278(4) (2000) G652–61. [PubMed: 10762620]

[30]. Rao R, Endotoxemia and gut barrier dysfunction in alcoholic liver disease, Hepatology 50(2) (2009) 638–44. [PubMed: 19575462]

[31]. Lamas-Paz A, Hao F, Nelson LJ, Vazquez MT, Canals S, Gomez Del Moral M, Martinez-Naves E, Nevzorova YA, Cubero FJ, Alcoholic liver disease: Utility of animal models, World J Gastroenterol 24(45) (2018) 5063–5075. [PubMed: 30568384]

[32]. Li X, Wang Z, Zou Y, Lu E, Duan J, Yang H, Wu Q, Zhao X, Wang Y, You L, He L, Xi T, Yang Y, Pretreatment with lipopolysaccharide attenuates diethylnitrosamine-caused liver injury in mice via TLR4-dependent induction of Kupffer cell M2 polarization, Immunol Res 62(2) (2015) 137–45. [PubMed: 25846584]

[33]. Lei N, Franken L, Ruzehaji N, Offenhauser C, Cowin AJ, Murray RZ, Flightless, secreted through a late endosome/lysosome pathway, binds LPS and dampens cytokine secretion, J Cell Sci 125(Pt 18) 4288–96. [PubMed: 22718342]

[34]. Adams DH, Ruzehaji N, Strudwick XL, Greenwood JE, Campbell HD, Arkell R, Cowin AJ, Attenuation of Flightless I, an actin-remodelling protein, improves burn injury repair via modulation of transforming growth factor (TGF)-beta1 and TGF-beta3, Br J Dermatol 161(2) (2009) 326–36. [PubMed: 19519830]

[35]. Rosa DF, Sarandy MM, Novaes RD, da Matta SLP, Goncalves RV, Effect of a high-fat diet and alcohol on cutaneous repair: A systematic review of murine experimental models, PloS one 12(5) (2017) e0176240. [PubMed: 28493875]

[36]. Rosa DF, Sarandy MM, Novaes RD, Freitas MB, do M. Carmo Gouveia Peluzio, R.V. Goncalves, High-Fat Diet and Alcohol Intake Promotes Inflammation and Impairs Skin Wound Healing in Wistar Rats, Mediators Inflamm 2018 (2018) 4658583. [PubMed: 30140168]

[37]. Gao B, Xu MJ, Bertola A, Wang H, Zhou Z, Liangpunsakul S, Animal Models of Alcoholic Liver Disease: Pathogenesis and Clinical Relevance, Gene Expr 17(3) (2017) 173–186. [PubMed: 28411363]

[38]. Ki SH, Park O, Zheng M, Morales-Ibanez O, Kolls JK, Bataller R, Gao B, Interleukin-22 treatment ameliorates alcoholic liver injury in a murine model of chronic-binge ethanol feeding: role of signal transducer and activator of transcription 3, Hepatology 52(4) (2010) 1291–300. [PubMed: 20842630]

[39]. Nielsen MJ, Veidal SS, Karsdal MA, Orsnes-Leeming DJ, Vainer B, Gardner SD, Hamatake R, Goodman ZD, Schuppan D, Patel K, Plasma Pro-C3 (N-terminal type III collagen propeptide) predicts fibrosis progression in patients with chronic hepatitis C, Liver Int 35(2) (2015) 429–37. [PubMed: 25308921]

Highlights

- Ethanol increases FLII protein levels and nuclear translocation *in vivo* and *in vitro*
- Ethanol disrupts FLII/NXN/MYD88 complex during ALD early progression
- NXN overexpression reverts ethanol effect on FLII and FLII/NXN/MYD88 complex status
- Ethanol increases FLII secretion into both mice plasma and cell culture medium
- FLII is a potential non-invasive biomarker for early detection of ALD in plasma

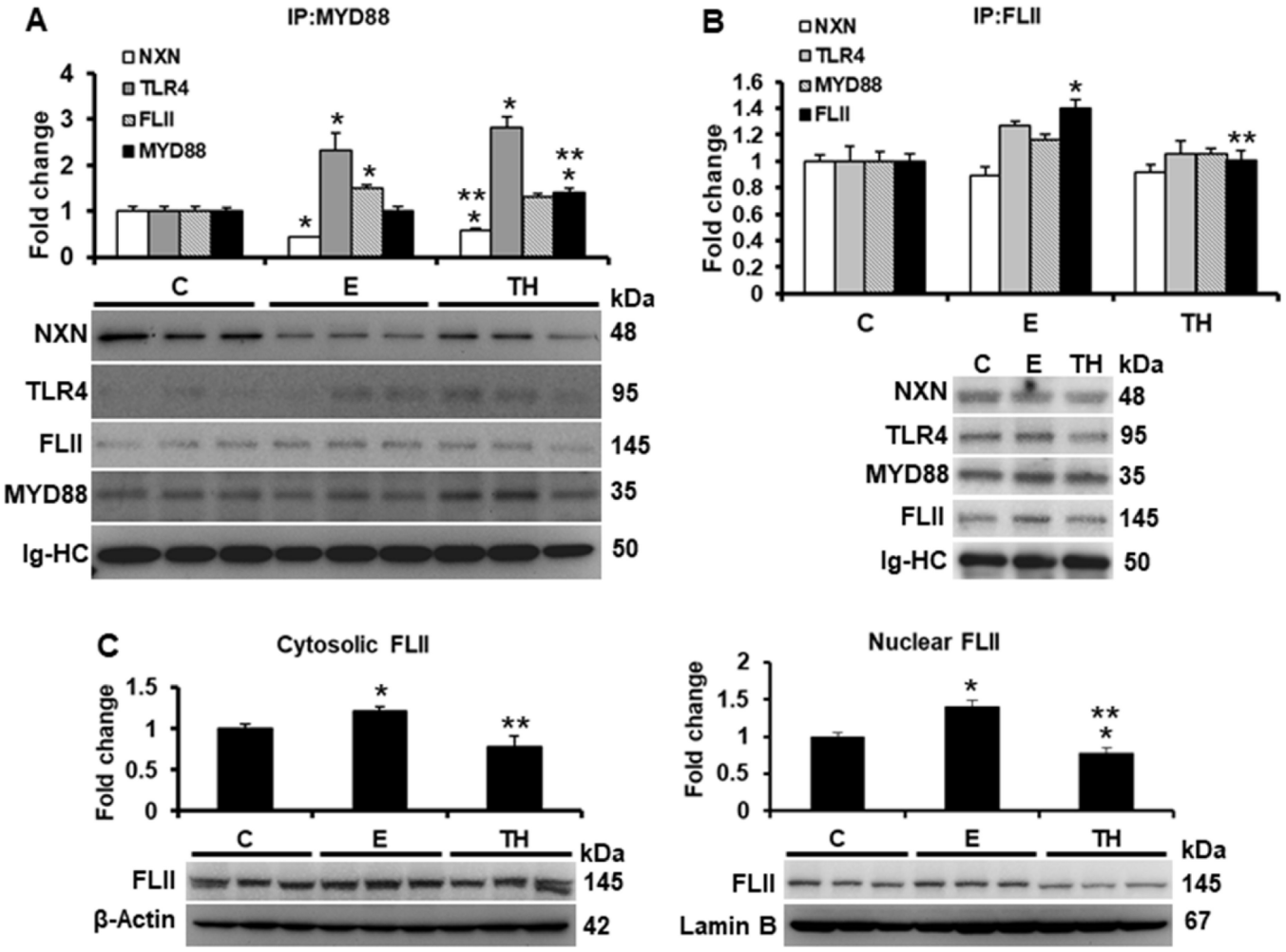

Fig. 1. Effect of ethanol on FLII/NXN/MYD88 complex and FLII status.

Total liver protein extracts were used for IP assays. (**A**) IP of MYD88 co-precipitated NXN, TLR4 and FLII proteins. Ethanol and TH model decreased 56% and 40% NXN/MYD88 interaction ratio, respectively, and induced 2.3 and 2.8 fold the MYD88/TLR4 interaction ratio, respectively. MYD88 precipitated level was increased 1.4 fold by TH model *vs* controls. (**B**) IP of FLII co-precipitated NXN, TLR4 and MYD88 proteins. FLII was precipitated 1.4 fold by ethanol *vs* controls but reverted by TH model. (**C**) Cytosolic and n=5 nuclear localization of FLII content. Levels of the house-keepings β-Actin and Lamin B were used to normalize cytosolic and nuclear FLII levels, respectively. All proteins were detected by western blot analyses. Densitometric analyses were used to quantify the spots. Immunoglobulin heavy chains (**Ig-HC**) used for IP (anti-MYD88 and anti-FLII) assays were detected and quantify to normalize precipitated protein levels. Bars values are expressed as fold change compared to controls and represent the mean ±SE. animals/group. Statistically different from *C and from **E group; p<0.05. **C**, Control; **E**, ethanol/binge; **TH**, ethanol/binge/LPS. n=5

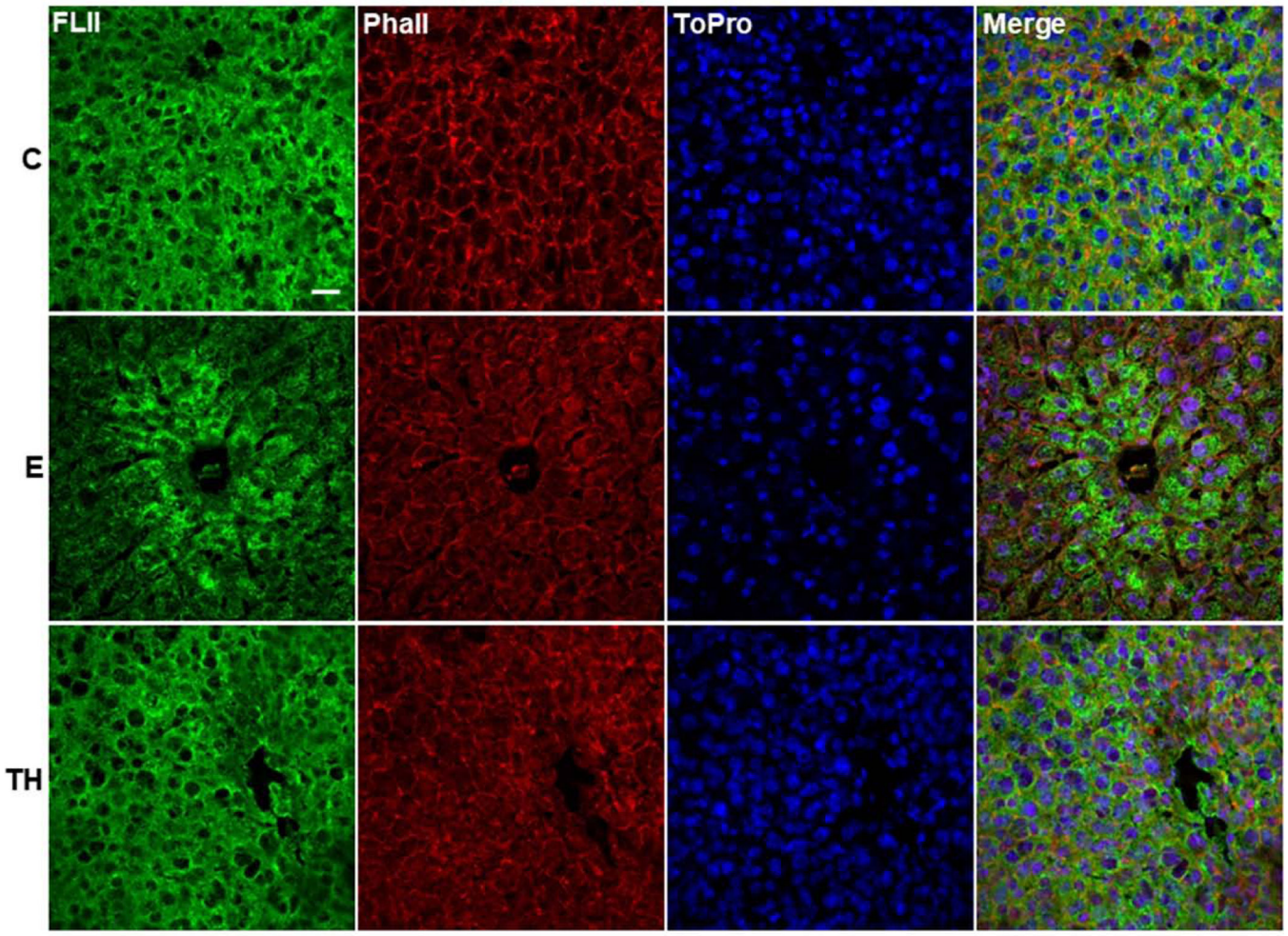

Fig. 2. Effect of ethanol on FLII localization in the hepatic tissue.

Immunodetection of FLII by IF analysis. FLII expression was stained in green, actin filaments were stained with phalloidin (red) and nuclei were stained with ToPro (blue). animals/group. White bar in group C represents 50 μm. Magnification: 63X. **C**, Control; **E**, ethanol/binge; **TH**, ethanol/binge/LPS.

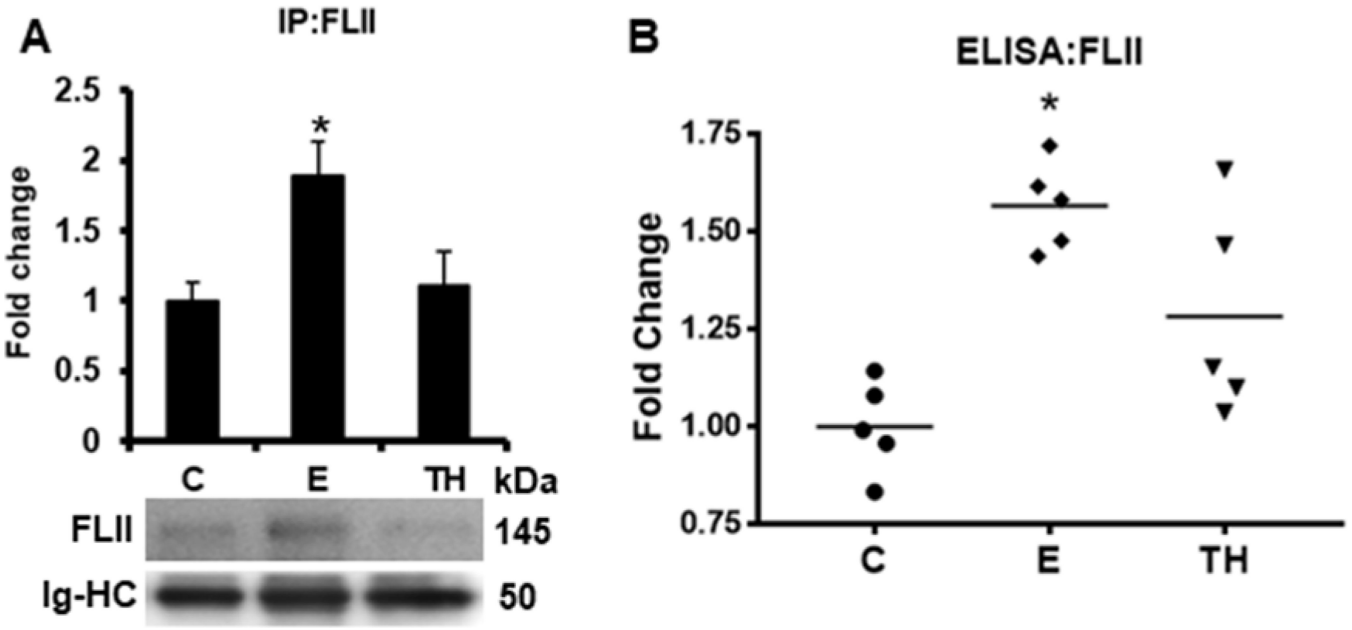

Fig. 3. Effect of ethanol on FLII secretion into mouse bloodstream.

FLII levels were detected in mice plasma by (**A**) IP and (**B**) ELISA assays as described in materials and methods section. Immunoglobulin heavy chains (**Ig-HC**) used for IP (anti-FLII antibody) assay were detected and quantify to normalize precipitated FLII levels. Bars values are expressed as fold change compared to controls and represent the mean ±SE. n = 5 animals/group. Statistically different from *C group; $p<0.05$. **C**, Control; **E**, ethanol/binge; **TH**, ethanol/binge/LPS.

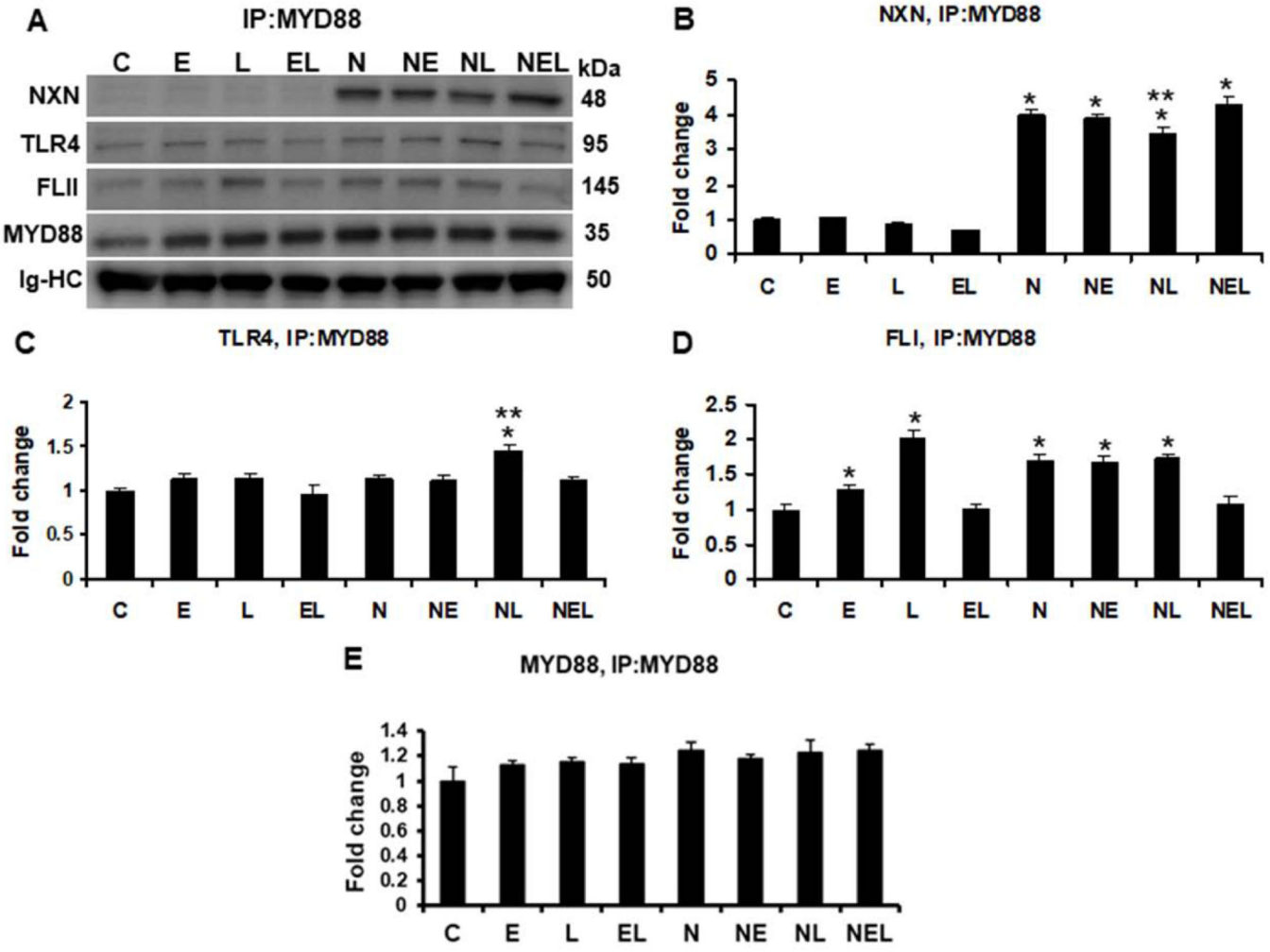

Fig. 4. IP of MYD88 and evaluation of ethanol effect on FLII/NXN/MYD88 complex *in vitro*.

(**A**) Western blot analyses were used to quantify NXN, FLII and TLR4 proteins co-immunoprecipitated with MYD88 protein. Densitometric quantification of (**B**) NXN, (**C**) TLR4, (**D**) FLII, and (**E**) MYD88 protein levels. NXN was co-precipitated more than 3 fold in NXN-transfected cells. LPS decreased 15% NXN/MYD88 interaction ratio but increased 1.4 fold MYD88/TLR4 interaction ratio in NXN overexpressing cells. Ethanol and LPS alone increased 1.3 and 2.0 fold, respectively, the MYD88/FLII binding ratio in untrasfected cells. NXN transfection itself promoted 1.7 ($p<0.001$) fold this binding ratio but ethanol plus LPS disrupted this interaction in untransfected cells. Total proteins from co-cultures were used for MYD88 immunoprecipitation. Immunoglobulin heavy chains (**Ig-HC**) used for IP (anti-MYD88 antibody) assay were detected and quantify to normalize all precipitated proteins. Bars values are expressed as fold change compared to controls and represent the mean ±SE. n=6 per group. Statistically different from *C and from **N groups; $p<0.05$. Groups: **C**, Control; **E**, Ethanol; **L**, LPS; and **EL**, Ethanol plus LPS, were transfected with EV and were called untransfected cells. **N**, NXN-transfected cells; these cells were also exposed to **E**, **L** and **EL** treatments and were identified as: **NE**, **NL** and **NEL**, respectively.

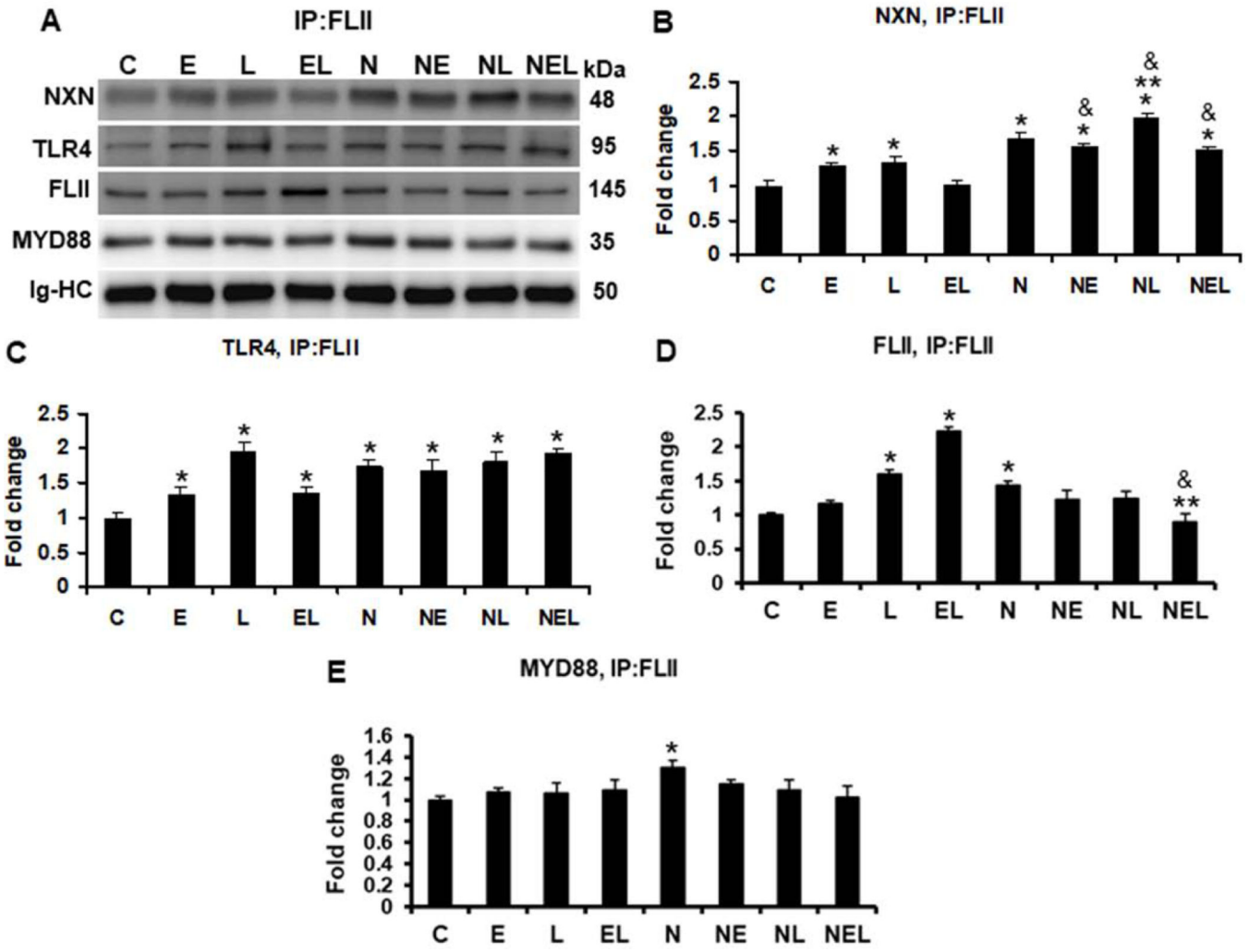

Fig. 5. IP of FLII and evaluation of ethanol effect on FLII/NXN/MYD88 complex *in vitro*.

(**A**) Western blot analyses were used to quantify MYD88, NXN, and TLR4 proteins co-immunoprecipitated with FLII protein. Densitometric quantification of (**B**) NXN, (**C**) TLR4, (**D**) FLII, and (**E**) MYD88 protein levels. Ethanol and LPS alone increased 1.3 fold NXN/FLII binding ratio but their combination reverted it in untransfected cells. This increment was induced 1.2 fold by LPS in NXN-transfected cells. Ethanol and LPS alone, and their combination increased 1.3, 1.9 and 1.3 fold, respectively, NXN/TLR4 binding ratio in untranfected cells FLII levels were increased more than 1.5 and 2.2 fold by LPS and by ethanol plus LPS, respectively, in untransfected cells but this levels were decreased 38% by ethanol plus LPS in NXN overexpressing cells. MYD88 levels increased 1.3 fold in NXN-transfected vs untransfected controls. Total proteins from co-cultures were used for FLII immunoprecipitation. Immunoglobulin heavy chains (**Ig-HC**) used for IP (anti-FLII antibody) assay were detected and quantify to normalize all precipitated proteins. Bars values are expressed as fold change compared to controls and represent the mean ±SE. n=6 per group. Statistically different from *C, from **N, and from &the same treatment in untransfected cells; p<0.05. Groups: **C**, Control; **E**, Ethanol; **L**, LPS; and **EL**, Ethanol

plus LPS, were transfected with EV and were called untransfected cells. **N**, NXN-transfected cells; these cells were also exposed to **E**, **L** and **EL** treatments and were identified as: **NE**, **NL** and **NEL**, respectively.

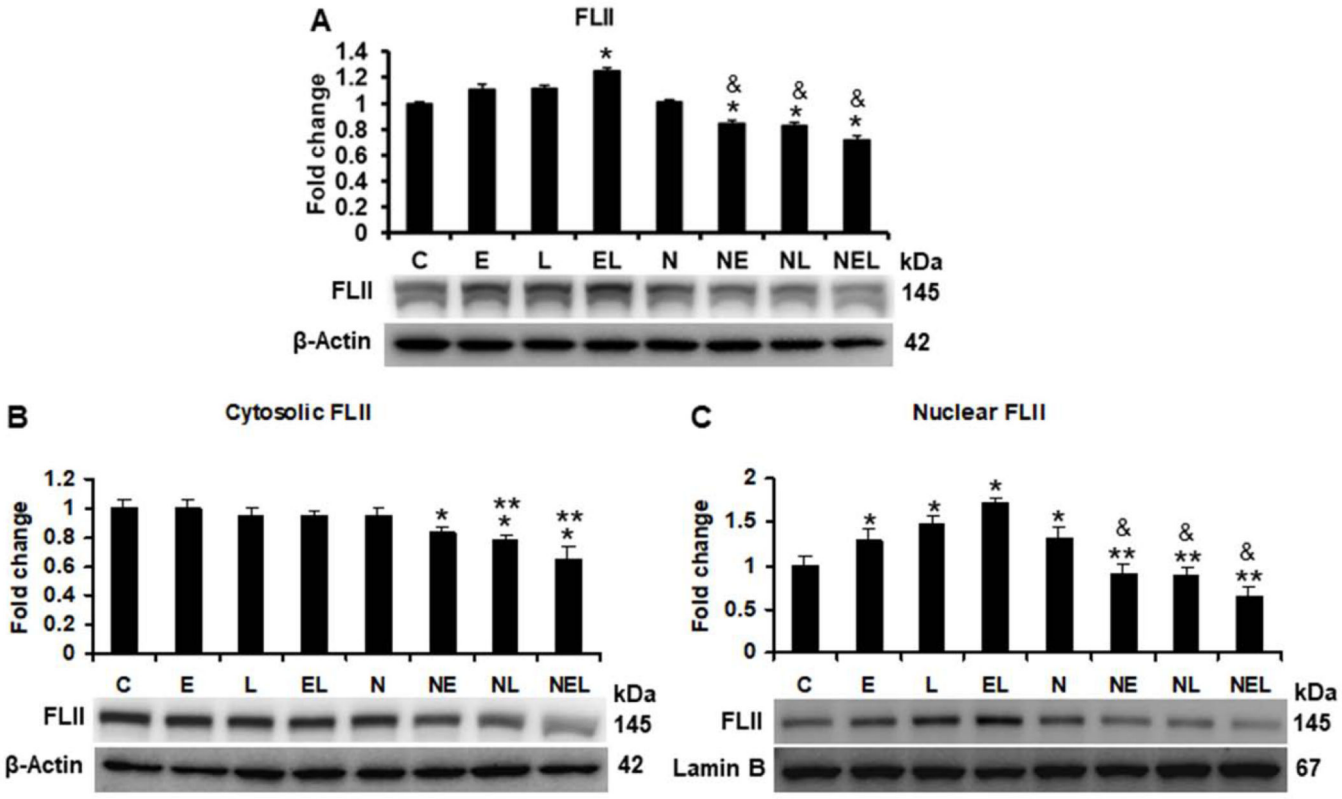

Fig. 6. Ethanol effect on FLII protein status *in vitro*.

(**A**) Total, (**B**) Cytosolic, and (**C**) Nuclear content of FLII. Co-cultures transfected either with empty (EV) or with NXN expression vector were treated with ethanol and/or LPS for 48 h. While total and cytosolic protein levels were normalized to the house-keeping β-Actin, that of nuclear protein levels were normalized to Lamin B levels. Bars values are expressed as fold change compared to controls and represent the mean ±SE. n=6 per group. Statistically different from *C, from **N, and from &the same treatment in untransfected cells; p<0.05. Groups: **C**, Control; **E**, Ethanol; **L**, LPS; and **EL**, Ethanol plus LPS, were transfected with EV and were called untransfected cells. **N**, NXN-transfected cells; these cells were also exposed to **E**, **L** and **EL** treatments and were identified as: **NE**, **NL** and **NEL**, respectively.

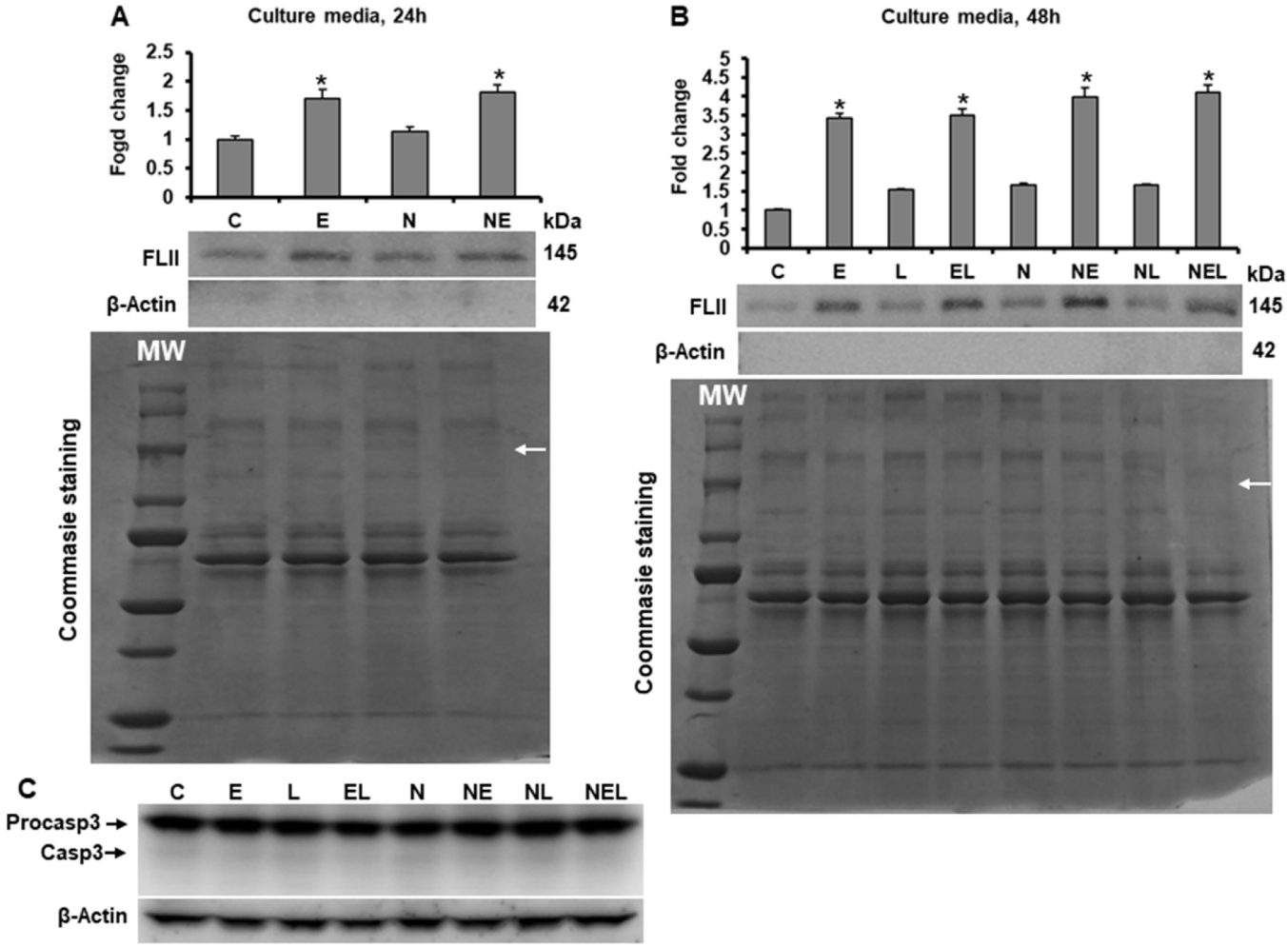

Fig. 7. Effect of ethanol on FLII secretion into cell culture medium.

Determination of FLII secretion after (**A**) 24 and (**B**) 48 h of ethanol and/or LPS exposition. Culture media were collected at indicated times and prepared as described in materials and methods section. β-Actin was detected to discard that secretion of FLII was due to cells breaking. Protein levels were normalized to Coommasie Blue-stained gels used as loading control. (**C**) Cleaved Caspase-3 (Casp3) was detected in total protein from co-cultures to discard that secretion of FLII was due to programmed cell death activation. Bars values are expressed as fold change compared to controls and represent the mean ±SE. n=6 group. Statistically different from *C group; p<0.05. White MW letters and arrows on Coommasie Blue-stained gels indicate protein Molecular Weights and FLII size location, respectively. Groups: **C**, Control; **E**, Ethanol; **L**, LPS; and **EL**, Ethanol plus LPS, were transfected with EV and were called untransfected cells. **N**, NXN-transfected cells; these cells were also exposed to **E**, **L** and **EL** treatments and were identified as: **NE**, **NL** and **NEL**, respectively.

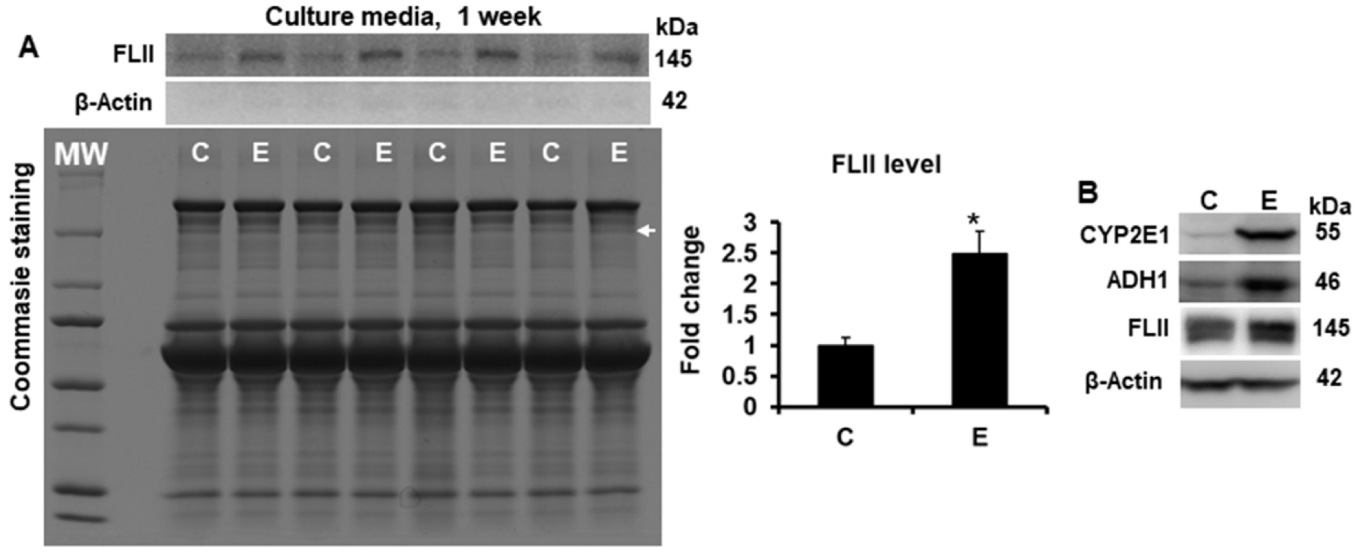

Fig. 8. Effect of ethanol on FLII secretion into cell culture medium after one week of ethanol exposition.

(**A**) Secretion of FLII into the culture medium. Culture media were collected one week after ethanol exposition and prepared as described in materials and methods section. Protein levels were normalized to Coommasie Blue-stained gels used as loading control. (**B**) Protein levels of CYP2E1, ADH1 and FLII. Total proteins were extracted from co-cultures after one week of ethanol exposition. To prevent cells death by the prolonged period of starvation time, ethanol was mixed in regular culture medium. Bars values are expressed as fold change compared to controls and represent the mean ±SE. n=6 per group. Statistically different from *C group; p<0.05. White MW letters and arrows on Coommasie Blue-stained gel indicate protein Molecular Weights and FLII size location, respectively. Groups: **C**, Control; **E**, Ethanol.

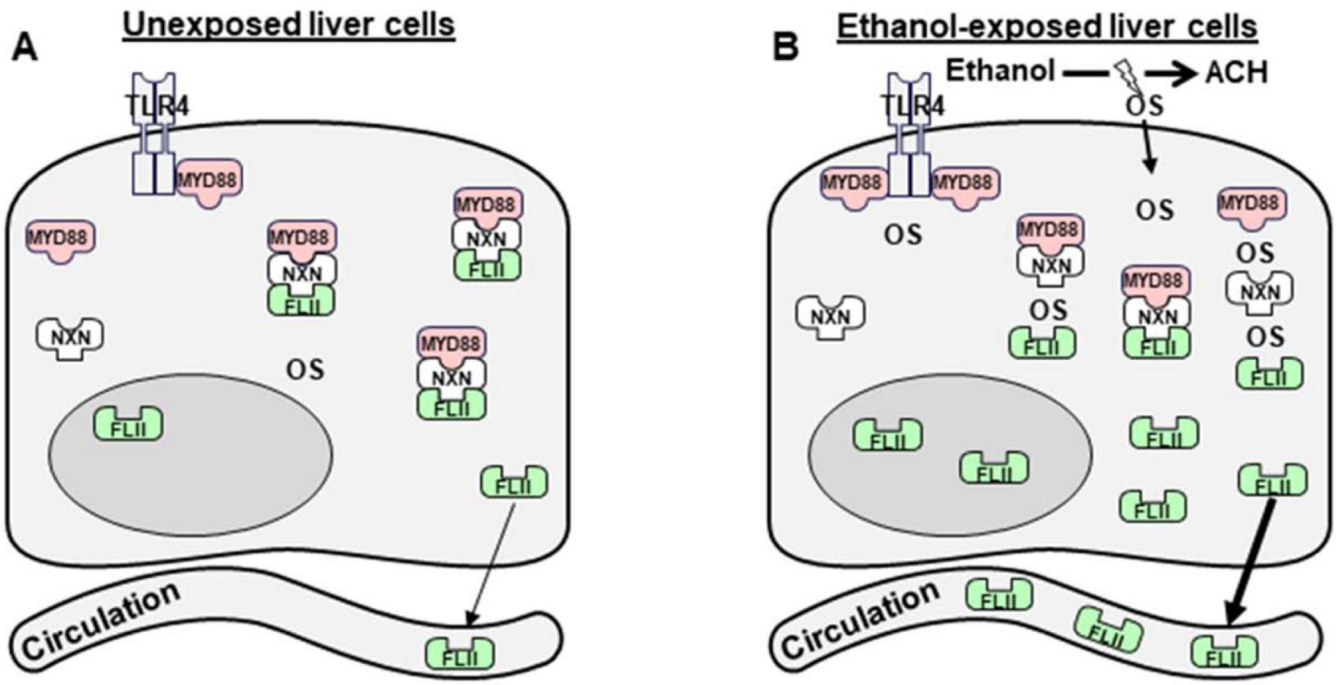

Fig. 9. Schematic representation of ethanol and/or LPS effects on FLII/NXN/MYD88 complex and FLII secretion.

It is well-known that ethanol metabolism mainly by ALD and CYP2E1 enzymes increases oxidative stress (OS) which is considered the primary mechanism of liver injury during ALD progression [3]. (**A**) Image shows basal status of OS, FLII, NXN, MYD88, and FLII/NXN/MYD88 complex in unexposed cells to ethanol effects. (**B**) Upon chronic ethanol exposition, OS levels increase and oxidize NXN disrupting FLII/NXN/MYD88 complex, and increasing FLII levels and secretion into the blood circulation. The complex might be differentially disrupted and MYD88 might increase its interaction with TLR4. Additionally, LPS administration partially reverts the effects of ethanol but NXN overexpression modifies the response of FLII/NXN/MYD88 complex to ethanol and/or LPS effects *in vitro*. The reversal effect of LPS might be due to the development of hepatic tolerance to neutralize the hyperactivation of TLR4/MYD88 signaling pathway.